Scientific Research Publishing

World Journal of Condensed Matter Physics, 2026, 16(4), 161-177
https://www.scirp.org/journal/wjcmp
ISSN Online: 2160-6927
ISSN Print: 2160-6919

Theoretical Anticipation of the Mixing Properties of Ag-Cu Melts at Different Temperatures

Nabin Kumar Roy[1], Prakash Ranjan Deen[2], Soni Kumari[3], Ajay Kumar Pandey[3], Jagdhar Mandal[4*], Indu Shekhar Jha[5]

[1]Department of Chemistry, Tilka Manjhi Bhagalpur University, Bhagalpur, India
[2]Department of Physics, Purnea College, Purnia, Purnea University, Purnia, India
[3]Department of Physics, Purnea University, Purnia, India
[4]Department of Physics, Tilka Manjhi Bhagalpur University, Bhagalpur, India
[5]Department of Physics, Mahendra Morang Adarsh Multiple Campus, Biratnagar, Nepal
Email: nabinkrroy@gmail.com; talk2deen@gmail.com; sonikrisharma2411@gmail.com; akpphysics01@gmail.com; *jmandal1284@gmail.com; isjha12345@gmail.com

How to cite this paper: Roy, N.K., Deen, P.R., Kumari, S., Pandey, A.K., Mandal, J. and Jha, I.S. (2026) Theoretical Anticipation of the Mixing Properties of Ag-Cu Melts at Different Temperatures. *World Journal of Condensed Matter Physics*, **16**, 161-177.
https://doi.org/10.4236/wjcmp.2026.164009

Received: October 1, 2026
Accepted: November 17, 2026
Published: November 20, 2026

Copyright © 2026 by author(s) and Scientific Research Publishing Inc.
This work is licensed under the Creative Commons Attribution International License (CC BY 4.0).
http://creativecommons.org/licenses/by/4.0/

Open Access

Abstract

The temperature and composition dependency of the thermodynamic, structural and transport properties of Ag-Cu melts has been theoretically analysed with the help of molecular interaction volume model (MIVM). For the computations of the mixing properties of Ag-Cu melts, the evaluation of the model parameters are required. The Newton-Raphson method is adopted for the estimation of the model parameters by employing the experimental data of activity coefficients of Ag and Cu in the infinite dilute solution region. The concentration dependence of the Gibbs excess free energy of mixing, Gibbs free energy of mixing, activity coefficients as well as activity of Ag-Cu melts at 1423 K, 1523 K and 1623 K has been analysed. The model parameters are also utilised to describe the concentration dependency of structural properties like concentration fluctuations as well as the short-range order parameter, and transport property such as the diffusivity ratio of Ag-Cu melts at 1423 K, 1523 K and 1623 K. The theoretical results of the mixing properties of Ag-Cu melts at 1423 K are compared with the interrelated experimental results available in the literature. The theoretical results exhibit good agreement with the available experimental results at 1423 K. The present theoretical analysis reveals that Ag-Cu melts are segregating in nature at 1423 K, 1523 K and 1623 K, and with the increase in temperature from 1423 to 1623 K, the segregation in Ag-Cu melts degrades. Again, the thermodynamic behaviour of Ag-Cu melts illustrates that Ag-Cu melt is a weakly segregating alloy.

Keywords

MIVM Model, Excess Free Energy of Mixing, Activity Coefficients, Short-Range Order Parameter, Concentration Fluctuations

1. Introduction

The phase diagram [1]-[3] of Ag-Cu molten alloy exhibits the presence of a simple eutectic around the composition of Ag, $x_{Ag} = 0.6$ *i.e.* the eutectic point of $Ag_{60}Cu_{40}$, which indicates the coexistence of the solid and liquid phases in thermal equilibrium. The concentration reliance of G_M^E (excess free energy of mixing), G_M (free energy of mixing), H_M (enthalpy of mixing), and S_M (entropy of mixing) is symmetric for Ag-Cu system at 1423 K. The activity of the components silver and copper *i.e.* a_{Ag} and a_{Cu} respectively, display the positive departures from the ideal mixing values indicating the segregating nature of Ag-Cu melts at 1423 K [4]. Again, the positive values of G_M^E and H_M in the entire region of Ag-composition illustrate the segregation in Ag-Cu melts at 1423 K, which stand for the existence of homo-coordination *i.e.* Ag-Ag and Cu-Cu atoms pairing as closest neighbours [4].

The Ag-Cu and Ag-Cu based ternary alloys are crucial in electro-technical and electronic industries, joining technologies (for e.g. soldering, welding) and brazing, aerospace etc. [5]-[7]. Therefore, Ag-Cu and Ag-Cu based ternary alloys are very important for researchers [2] [3] [5]-[11] to understand their mixing behaviour of thermophysical properties such as phase diagram, thermodynamic properties, structural properties, and transport property. However, the analysis of the thermodynamic, structural, transport and surface propertiges for Ag-Cu melts at different temperatures is scanty in the literature.

In present study, MIVM [12] is employed to accesses the thermodynamic properties (G_M^E, G_M, activity), microscopic properties namely concentration fluctuations, $S_{cc}(0)$ as well as short-range order parameter, SRO, α_1, and transport property (diffusivity, D) with respect to the composition at different temperature for Ag-Cu melts. The structural properties like $S_{cc}(0)$ has been employed to explain the excess stability function (E^{XS}) of Ag-Cu melts at different temperatures.

The MIVM represents a statistical mechanical model which is successfully employed to investigate the thermodynamic properties like G_M^E, G_M, H_M, S_M, activity coefficient (γ_i), activity (a) as well as surface properties of several binary alloys namely Bi-Sn, Ca-X (X = Ag, Bi, In, Pb, Sn, Tl, Zn), Zn-Bi, Ni-Pd, Ti-Al, Fe-Mn, Zn-Cd, Pb-Bi, Cd-Tl etc. [13]-[21] and ternary alloys namely Pb-Sn-Sb, Sn-Ag-Au, In-Bi-Sb etc. [22]-[24]. However, the analysis of $S_{cc}(0)$ and α_1 as well as E^{XS} of the binary melts is insufficient in the literature. Therefore, the present theoretical research is focused on the theoretical anticipation of the thermodynamic properties like G_M^E, G_M, γ_i, a, structural properties like $S_{cc}(0)$, α_1 and excess stability (E^{XS}) as well as the transport property *i.e.* diffusivity ratio (D_M/D_{id}) of Ag-Cu melts at various temperatures.

2. Formalism

The present research work deals with the theoretical approach to the mixing properties like thermodynamic, microscopic and transport properties of the Ag-Cu melts at different temperatures on employing MIVM model. The present section exhibits the basic concept of MIVM model.

2.1. Thermodynamic Properties *i.e.* Excess Free Energy of Mixing, G_M^E, Free Energy of Mixing, G_M, Activity Coefficient, γ_υ and Activity, $a_\upsilon(\upsilon = i, j)$ of Binary Molten Alloys

The MIVM is a fluid-based model introduced by Tao [12] on employing statistical thermodynamics, fluid-phase equilibria and the fundamental concept of the non-random exchange of liquid molecules. The molecular excess free energy of mixing of a binary molten alloy $i-j$ may be expressed as [12]

$$\frac{G_M^E}{RT} = x_i \ln\left(\frac{V_{mi}}{x_i V_{mi} + x_j V_{mj} A_{ji}}\right) + x_j \ln\left(\frac{V_{mj}}{x_j V_{mj} + x_i V_{mi} A_{ij}}\right) - \frac{x_i x_j}{2}\left(\frac{Z_i A_{ji} \ln A_{ji}}{x_i + x_j A_{ji}} + \frac{Z_j A_{ij} \ln A_{ij}}{x_j + x_i A_{ij}}\right) \tag{1}$$

where, x_i and x_j are the compositions of the component *i* and *j* respectively; Z_i and Z_j indicate the first coordination numbers of the component *i* and *j* respectively; A_{ij} and A_{ji} are the energy interaction parameters, which are dependent on the temperature but independent on the pressure and concentration. The energy interaction parameters are expressed as [12]

$$A_{ji} = \exp\left[-\frac{\varepsilon_{ji} - \varepsilon_{ii}}{kT}\right] \text{ and } A_{ij} = \exp\left[-\frac{\varepsilon_{ij} - \varepsilon_{jj}}{kT}\right] \tag{2}$$

where, ε_{ii}, ε_{jj} and ε_{ji} = potential energies for the pairs *i-i*, *j-j* and *i-j* respectively with $\varepsilon_{ji} = \varepsilon_{ij}$; k = Boltzmann constant and T = temperature (in K) of the pure components in liquid state.

The partial molar free energy and molar excess free energy are related as [12]

$$G_M^{\tilde{E}} = RT \ln \gamma_i = G_M^E + \delta\left(\frac{\partial G_M^E}{\partial x_i}\right)_{T,P,x[i,N]} - \sum_{j=1}^{N}\left(\frac{\partial G_M^E}{\partial x_i}\right)_{T,P,x[j,N]} \tag{3}$$

The above equation satisfies the conditions that when $i \neq N$, $\delta = 1$; as well as $i = N$, $\delta = 0$. Again, $x[i,N]$ refers to the variables x_j and x_N where, $x_N = 1 - \sum_{j=1}^{N-1} x_j$.

Now, the activity coefficients for both the components i and j of a binary solution are, respectively, represented by [12]

$$\ln \gamma_i = \ln\left(\frac{V_{mi}}{x_i V_{mi} + x_j V_{mj} A_{ji}}\right) + x_j\left(\frac{V_{mj} A_{ji}}{x_i V_{mi} + x_j V_{mj} A_{ji}} - \frac{V_{mi} A_{ji}}{x_j V_{mj} + x_i V_{mi} A_{ij}}\right) - \frac{x_j^2}{2}\left(\frac{Z_i A_{ji}^2 \ln A_{ji}}{\left(x_i + x_j A_{ji}\right)^2} + \frac{Z_j A_{ij} \ln A_{ji}}{\left(x_j + x_i A_{ij}\right)^2}\right) \tag{4}$$

and

$$\ln\gamma_j = \ln\left(\frac{V_{mj}}{x_j V_{mj} + x_i V_{mi} A_{ij}}\right) - x_i\left(\frac{V_{mj}A_{ji}}{x_i V_{mi} + x_j V_{mj} A_{ji}} - \frac{V_{mi}A_{ij}}{x_j V_{mj} + x_i V_{mi} A_{ij}}\right) - \frac{x_i^2}{2}\left(\frac{Z_j A_{ij}^2 \ln A_{ij}}{\left(x_j + x_i A_{ij}\right)^2} + \frac{Z_i A_{ji} \ln A_{ji}}{\left(x_i + x_j A_{ji}\right)^2}\right) \tag{5}$$

The first co-ordination number of element of the binary system can be determined from the relation [12]

$$Z_i = \frac{4\sqrt{2\pi}}{3}\left(\frac{r_{mi}^3 - r_{oi}^3}{r_{mi} - r_{oi}}\right)\rho_i r_{mi} \exp\left(\frac{\Delta H_{mi}\left(T_{mi} - T\right)}{Z_C R T_{mi}}\right) \tag{6}$$

with ΔH_{mi} = enthalpy of the component at melting temperature (T_{mi}), and Z_C represents the co-ordination number for closed packed structure (which is usually taken to be 12); $\rho_i = N_i V_i = \dfrac{0.6022}{V_{mi}}$, molecular number density; r_{mi} and r_{oi} = initial value and first peak value respectively of the radial distribution function for molten element i (near melting temperature), and R is well known universal gas constant. The radial distances are given by

$$r_{oi} = 0.918 d_{covi} \quad \text{and} \quad r_{mi} = \sigma_i \tag{7}$$

where, σ_i and d_{covi} = atomic diameter as well as atomic covalent diameter.

The relations for activity coefficient of both the components for the alloy in infinite dilute solution region such as x_i or $x_i \to 0$, are, respectively, represented by

$$\ln\gamma_i^{\infty} = 1 - \ln\left(\frac{V_{mj}A_{ji}}{V_{mi}}\right) - \frac{V_{mi}A_{ji}}{V_{mj}} - \frac{1}{2}\left(Z_i \ln A_{ji} + Z_j A_{ij} \ln A_{ij}\right) \tag{8}$$

and

$$\ln\gamma_j^{\infty} = 1 - \ln\left(\frac{V_{mi}A_{ij}}{V_{mj}}\right) - \frac{V_{mj}A_{ji}}{V_{mi}} - \frac{1}{2}\left(Z_j \ln A_{ij} + Z_i A_{ji} \ln A_{ji}\right) \tag{9}$$

Again, the expressions for the activity in terms of activity coefficients for species i and j are given by [4]

$$a_i = \gamma_i x_i \tag{10a}$$

$$a_j = \gamma_j x_j \tag{10b}$$

2.2. Microscopic Properties *i.e.* $S_{cc}(0)$, α_1, Excess Stability Function, E^{XS} and Diffusivity, D of a Binary Molten Alloy

The $S_{cc}(0)$ and α_1 play vital role for explaining the nature of interatomic interactions existing in a binary melt [4]. The condition $S_{cc}(0) < S_{cc}^{id}(0)$ represents the unlike atoms ($i-j$) interactions in the liquid melts and the system is ordering in nature. Similarly, $S_{cc}(0) > S_{cc}^{id}(0)$ describes the segregation in the molten system *i.e.* like atoms ($i-i$ or $j-j$) interactions exists in the system [4].

The $S_{cc}(0)$ is related to G_M as [4], [25]

$$S_{cc}(0) = RT\left(\frac{\partial^2 G_M}{\partial x_i^2}\right)^{-1}_{T,P,N} = RT\left(\frac{\partial^2 G_M}{\partial x_j^2}\right)^{-1}_{T,P,N} \tag{11}$$

where,

$$G_M = G_M^E + G_M^{id} \tag{12}$$

$$\Rightarrow G_M = G_M^E + RT\left[x_i \ln x_i + x_j \ln x_j\right] \tag{13}$$

Equations (1), (11) and (13) yield

$$S_{cc}(0) = \frac{x_i x_j}{1 + x_i x_j f\left(x_i x_j\right)} \tag{14}$$

where,

$$f\left(x_i, x_j\right) = \frac{V_{mj}A_{ji} - V_{mi}}{x_i V_{mi} + x_j V_{mj} A_{ji}} + \frac{V_{mi}A_{ij} - V_{mj}}{x_j V_{mj} + x_i V_{mi} A_{ij}} + \frac{V_{mj}A_{ji}\left(V_{mj}A_{ji} - V_{mi}\right)}{\left(x_i V_{mi} + x_j V_{mj} A_{ji}\right)^2} + \frac{V_{mi}A_{ij}\left(V_{mi}A_{ij} - V_{mj}\right)}{\left(x_j V_{mj} + x_i V_{mi} A_{ij}\right)^2} + \left[\frac{Z_i A_{ji}^2 \ln A_{ji}}{\left(x_i + x_j A_{ji}\right)^3} + \frac{Z_j A_{ij}^2 \ln A_{ij}}{\left(x_j + x_i A_{ij}\right)^3}\right] \tag{15}$$

For ideal mixing condition, $G_M^E = 0$, Equation (12) reduces to $G_M = G_M^{id}$. Therefore, Equation (14) and (15) provide

$$S_{cc}^{id}(0) = x_i x_j \tag{16}$$

The above equation is used to compute the ideal value of $S_{cc}(0)$.

Again, the $S_{cc}(0)$ and thermodynamic activity of a molten system, are related as [4] [26] [27]

$$S_{cc}(0) = a_i x_j \left(\frac{\partial a_i}{\partial x_i}\right)^{-1} = a_j x_i \left(\frac{\partial a_j}{\partial x_j}\right)^{-1} \tag{17}$$

The experimental results of activities are used to evaluate the values of $S_{cc}(0)$ of a binary alloy, which are recognised as the experimental data of $S_{cc}(0)$ [4] [25] [26]

The SRO, α_1 [27] [28] in terms of $S_{cc}(0)$ may be expressed as [4], [29]

$$\alpha_1 = \frac{S-1}{S(Z-1)+1} \text{ , where } S = \frac{S_{cc}(0)}{S_{cc}^{id}(0)} \tag{18}$$

In Equation (18) Z denotes the coordination number in the first-neighbour shell. It should be pointed out that the value of Z is taken to be 10.

Equation (18) discloses that α_1 = positive for segregating systems, α_1 = negative for ordering systems and α_1 = 0 for ideal melts.

Now, $S_{cc}(0)$ can be used to determine E^{XS} [4] [30] from the relation:

$$\frac{E^{XS}}{RT} = \left(S_{cc}(0)\right)^{-1} - \left(S_{cc}^{id}(0)\right)^{-1} \tag{19}$$

Obviously, E^{XS} may be positive or negative or zero depending upon whether

the system is ordering or segregating or ideal in nature in accordance with $S_{cc}(0) < S_{cc}^{id}(0)$ or $S_{cc}(0) > S_{cc}^{id}(0)$ or $S_{cc}(0) = S_{cc}^{id}(0)$ respectively.

The transport property namely diffusivity is found to be an important parameter to visualize the mixing behaviour at the microscopic level of a binary solution. For a binary solution, the diffusivity ratio is expressed as [31] [32].

$$\frac{D_M}{D_{id}} = \frac{S_{cc}^{id}(0)}{S_{cc}(0)} \tag{20}$$

where, D_M and D_{id} refer to the mutual diffusion coefficient of the system and intrinsic diffusion coefficient of ideal system respectively. Now, D_{id} is expressed as

$$D_{id} = x_i D_j + x_j D_i \tag{21}$$

where, D_i and D_j are known as self-diffusion coefficients of the pure i and j respectively.

The Equation (20) illustrates that $D_M / D_{id} > 1$ for ordered melt, $D_M / D_{id} < 1$ for segregating melt and $D_M / D_{id} = 1$ for ideal system.

3. Results and Discussions

The analytical equations deduced in the structure of MIVM for various properties of binary melts, are employed to compute the theoretical results relative to the concentration for Ag-Cu melts at different temperatures.

3.1. G_M^E, G_M, γ_μ and $a_\mu (\mu = i, j)$ of Ag-Cu Melts at 1423 K

The computations of G_M^E, G_M, γ_μ and activity, $a_\mu (\mu = i, j)$, require certain input parameters like ΔH_{mi}, σ_i, r_{oi} and V_{mi} for each component of the alloy, which are listed in **Table 1** [33] .The values of $Z_i\ (i = Ag)$ and $Z_j\ (j = Cu)$ estimated from Equation (6) are reported in **Table 2**. The Newton—Raphson method is employed to approximate the parameters A_{ji} and A_{ij} by the simultaneous solution of Equations (8) and (9). For this, the values of γ_{Ag}^{∞} and γ_{Cu}^{∞} are taken to be 3.375 and 3.406 respectively for Ag-Cu systems at 1423 K [1]. The values of A_{ji} and A_{ij} are found to be 0.7310 and 0.7747 respectively. It should be pointed out that these values of A_{ji} and A_{ij} are found to be not suitable during calculations for various thermodynamic functions of Ag-Cu melts at 1423 K. Therefore, the values of A_{ji} and A_{ij} are adjusted in order to achieve a well matching between the theory and experiment [1] for the G_M^E of Ag-Cu melts at 1423 K. The reasonable values of A_{ji} and A_{ij} are also mentioned in **Table 2**.

Table 1. Input parameters for pure Ag and Cu [33].

Metal,i	ΔH_{mi} (KJ/mol)	σ_i ($\times 10^{-8}$cm)	r_{oi} ($\times 10^{-8}$ cm)	V_{mi} (cm^3/mol)
Ag	11.09	2.82	2.34	11.6[1+0.98×10^{-4}(T-1233.65)]
Cu	13.00	2.50	2.06	7.94[1+1.0×10^{-4}(T-1356)]

Table 2. Values of A_{ij}, A_{ji}, Z_i and Z_j for the of Ag-Cu molten system at various temperatures.

i-j	*T*(K)	A_{ij}	A_{ji}	Z_i	Z_j
Ag-Cu	1423	0.9025	0.8821	9.62	9.85
	1523	0.9086	0.8894	9.53	9.75
	1623	0.9140	0.8958	9.44	9.66

The theoretical results of G_M^E/RT and G_M/RT computed using Equations (1) and (13) in terms of Ag -composition for Ag-Cu melts at 1423 K illustrate excellent matching with the correlated experimental results [1] as shown in **Figure 1**. In composition region, x_{Ag} = 0.1 to 0.9, G_M^E/RT has positive value at each concentration with maxima at the composition, x_{Ag} = 0.5 *i.e.* 0.2974 (Theory) and 0.2976 (Experiment). Thus, MIVM successfully describes the symmetry in G_M^E/RT with respect to composition and segregating nature of Ag-Cu melts at 1423 K. Again, G_M/RT - x_{Ag} isotherm depicted in **Figure 1**, illustrates the symmetric behaviour of G_M/RT for Ag-Cu melts at 1423 K because G_M/RT are minimum at x_{Ag} = 0.5, *i.e.* –0.3958 (Theory) and –0.3959 (Experiment). Further, the magnitude of G_M/RT advocates that Ag-Cu melt at 1423 K is a feebly segregating alloy [4].

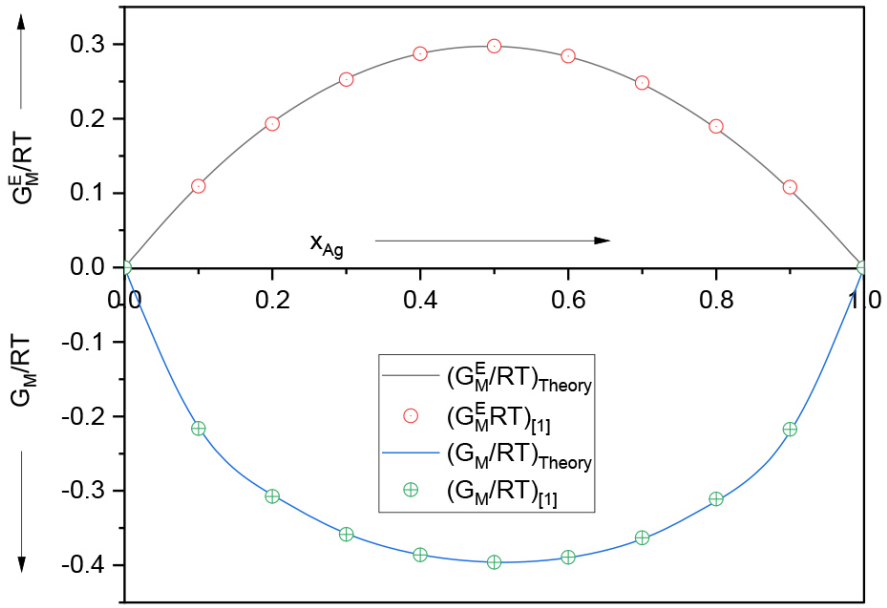

Figure 1. (G_M^E/RT and G_M/RT) vs x_{Ag} for Ag-Cu melts at 1423 K.

The theoretical data of γ_{Ag} and γ_{Cu} calculated using Equations (4) and (5) respectively in terms of Ag-composition indicate excellent agreement with the concerned experimental data [1] as shown in **Figure 2**.

Equations (10a) and (10b) are used to evaluate the values of a_{Ag} and a_{Cu} respectively, with respect to the concentration of Ag. **Figure 3** exhibits the well similarity between theory and experiment [1] in the complete composition range of Ag from 0.1 to 0.9. Again, the positive departures of a_{Ag} and a_{Cu} from Raoults' law confirm the segregation in Ag-Cu melts at 1423 K [4].

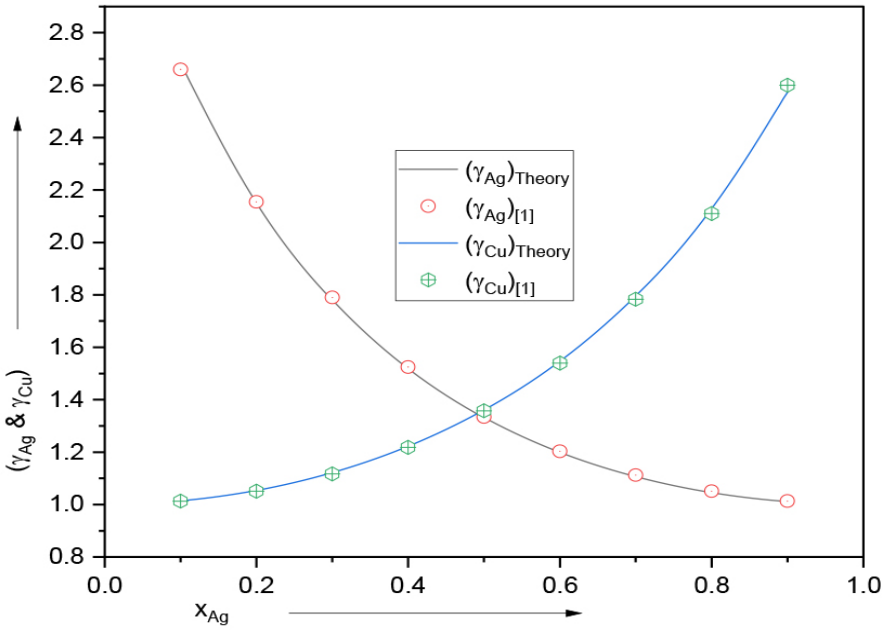

Figure 2. (γ_{Ag} and γ_{Cu}) vs x_{Ag} for Ag-Cu melts at 1423 K.

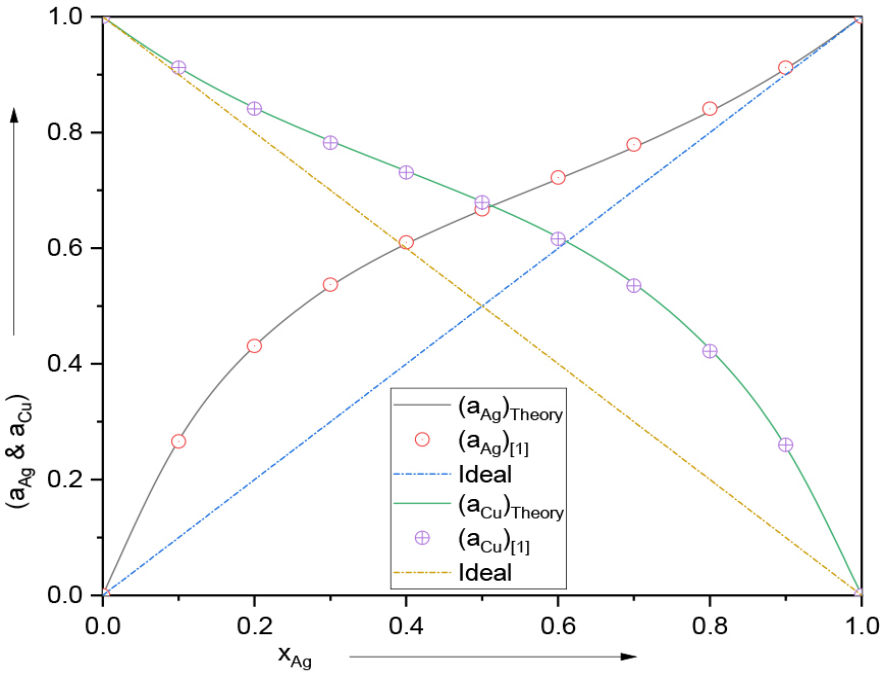

Figure 3. (a_{Ag} and a_{Cu}) vs x_{Ag} for Ag-Cu melts at 1423 K.

Therefore, the agreement between the theoretical and concerned experimental data of the activity for Ag-Cu melts at 1423 K, validates the estimated values of A_{ji} and A_{ij}.

3.2. $S_{cc}(0)$ of Ag-Cu Melts at 1423 K

Figure 4 illustrates the theoretical data of $S_{cc}(0)$ as a function of composition of

Ag for Ag-Cu melts at 1423 K computed via Equations (14) and (15). Figure 4 describes a well harmony between the theoretical data and concerned experimental data of $S_{cc}(0)$ [1] in the Ag- composition range from 0.1 to 0.9. The maximum values of $S_{cc}(0)$ are 0.650 (Theory) and 0.661 (Experiment) both at x_{Ag} = 0.5. This shows the symmetry in $S_{cc}(0)$ with respect to composition for Ag-Cu melts at 1423 K. Further, $S_{cc}(0) > S_{cc}(0)^{id}$ (included in Figure 4) at each composition which justifies the segregating behaviour of Ag-Cu molten alloys at 1423 K [4].

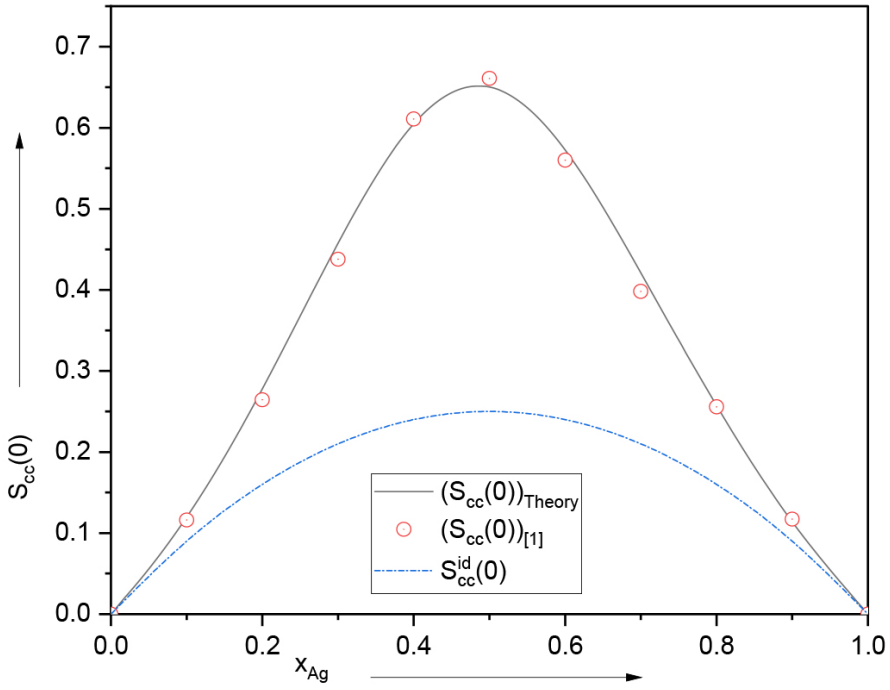

Figure 4. $S_{cc}(0)$ vs x_{Ag} for Ag-Cu melts at 1423 K.

The standard error is calculated by Equation (22) and presented in Table 3.

$$\text{Standard error}\left(S_i^*\right) = \pm\left[\frac{1}{n}\sum_{i=1}^{n}\left(a_{i,Expt} - a_{i,Pre}\right)^2\right]^{1/2} \tag{22}$$

Table 3. Standard error.

S^*	G_M^E/RT	G_M^E/RT	γ_{Ag}	γ_{Cu}	a_{Ag}	a_{Cu}	$S_{cc}(0)$
	0.00182%	0.00183%	0.00940%	0.01203%	0.00283%	0.00273%	0.01263%

3.3. G_M^E, G_M, a_{Ag}, a_{Cu}, $S_{cc}(0)$, E^{XS}, α_1 and D_M/D_{id} of Ag-Cu Melts at Different Temperatures

It should be pointed out that the present theoretical model (MIVM) can be used to analyse the thermodynamic properties of binary liquid alloys at various temperatures. Thus, MIVM model is employed for the concentration and temperature dependence of G_M^E, G_M, a_{Ag}, a_{Cu}, $S_{cc}(0)$, E^{XS}, α_1 and D_M/D_{id} for Ag-

Cu melts at 1423 K, 1523 K and 1623 K. The required input parameters are cited in Table 1 and Table 2. The values of parameters A_{ji} and A_{ij} are computed at required temperature (TK) by the equations [12]:

$$-\frac{\varepsilon_{ji}-\varepsilon_{ii}}{kT}=T\ln A_{ji}(T)=T_0\ln A_{ji}(T_0)$$

$$A_{ji}(T)=\exp\left(\frac{T_0\ln A_{ji}(T_0)}{T}\right) \tag{23a}$$

and

$$-\frac{\varepsilon_{ij}-\varepsilon_{jj}}{kT}=T\ln A_{ij}(T)=T_0\ln A_{ij}(T_0)$$

$$A_{ij}=\exp\left(\frac{T_0\ln A_{ij}(T_0)}{T}\right) \tag{23b}$$

where, T_0 = 1423 K

The values of A_{ji} and A_{ij} at various temperatures are also listed in Table 2.

The theoretical analysis of G_M^E/RT and G_M/RT for Ag-Cu melts with respect to the Ag- composition at 1423 K, 1523 K and 1623 K are presented in Figure 5. It is observed that both G_M^E/RT and G_M/RT indicate the symmetric behaviour relative to the composition for Ag-Cu melts at the temperatures from 1423 - 1623 K. Again, G_M^E/RT displays the declination with the upgradation of the temperature from 1423 - 1623 K at each composition with maxima at x_{Ag} = 0.5 *i.e.* 0.2974, 0.2746, and 0.2552 at 1423 K, 1523 K, and 1623 K respectively in Ag- composition from 0.1 to 0.9. The theoretical values of G_M/RT for Ag-Cu systems degrade *i.e.* the negative values of G_M/RT upgrade due to the elevation temperature from 1423 - 1623 K in whole range of x_{Ag} having minima at *i.e.* –0.3958, –0.4186 and –0.4379.

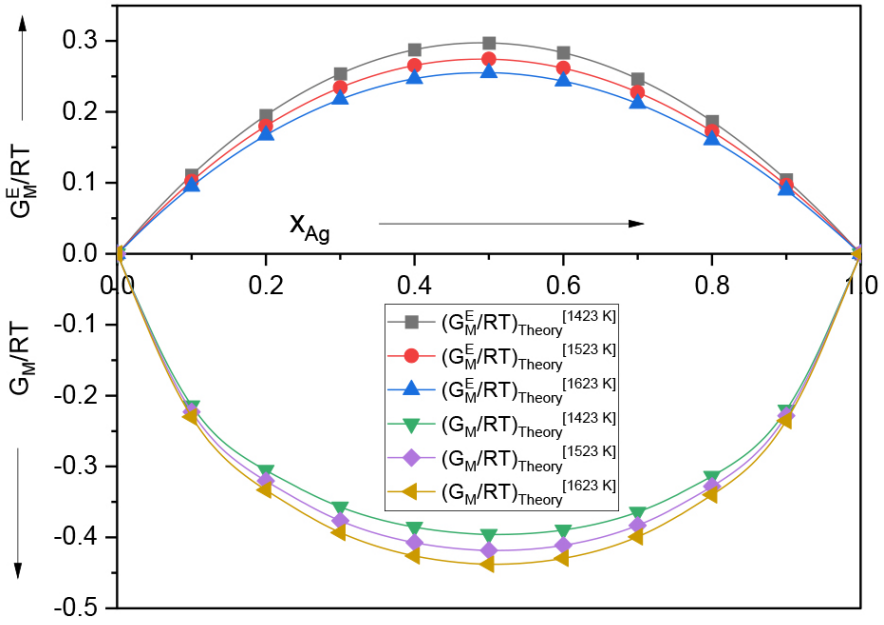

Figure 5. (G_M^E/RT and G_M/RT) vs x_{Ag} for Ag-Cu melts at 1423, 1523 & 1623 K.

all at x_{Ag} = 0.5, for 1423 K, 1523 K and 1623 K respectively. Therefore, the temperature reliance of G_M^E/RT and G_M/RT for Ag-Cu melts shows the decrease in the segregating nature with the rise in temperature from 1423 - 1623 K.

The activities of Ag and Cu *i.e.* a_{Ag} and a_{Cu} for Ag-Cu melts are calculated relative to the Ag- composition at 1423 K, 1523 K and 1623 K using the computed values γ_{Ag} and γ_{Cu} respectively. The $a_\mu(\mu = Ag, Cu)$ composition isotherms as mentioned in Figure 6, indicate that the positive departures of a_{Ag} and a_{Cu} from linearity gradually decrease with the rise in temperature from 1423 - 1623 K. This discloses the degradation of the segregating behaviour of Ag-Cu melts when temperature rises from 1423 - 1623 K.

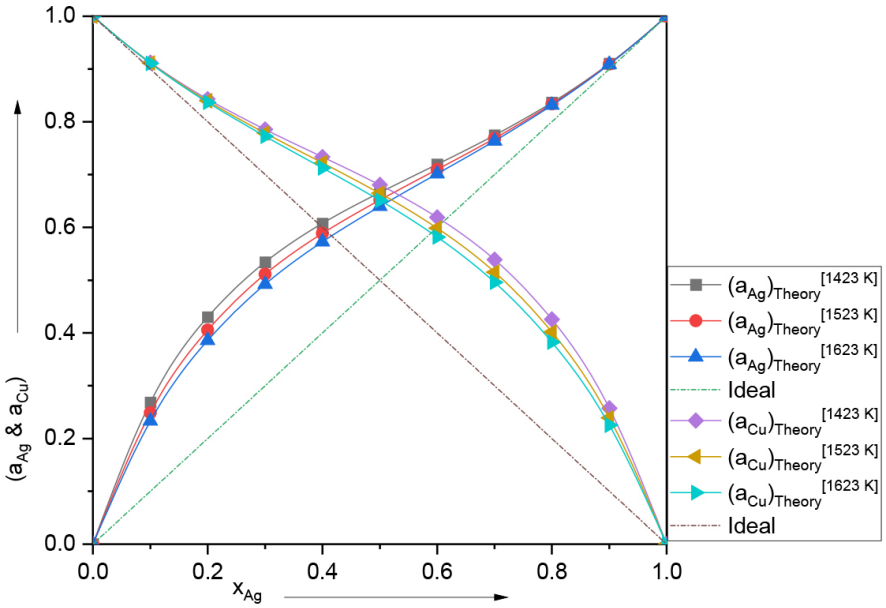

Figure 6. (a_{Ag} and a_{Cu}) vs x_{Ag} for Ag-Cu melts at 1423, 1523 & 1623 K.

The theoretical data of $S_{cc}(0)$ at 1423 K, 1523 K and 1623 K for Ag-Cu melts are depicted in Figure 7 along with $S_{cc}^{id}(0)$. Obviously, $S_{cc}(0) > S_{cc}^{id}(0)$ at each composition of Ag in the range from 0.1 to 0.9 at each temperature under consideration and the values of $S_{cc}(0)$ show the declination with the elevation of temperature from 1423 - 1623 K. However, the declination of $S_{cc}(0)$. is not distinct in the lower concentration as well as higher concentration region of Ag. Therefore, the present theoretical investigation reveals that the segregating behaviour of Ag-Cu melts gradually decreases in the temperature region, 1423 - 1623 K. Further the symmetry in $S_{cc}(0)$ as a function of concentration is mainined in the temperature region 1423 - 1623 K because the values of $S_{cc}(0)$ are maximum at x_{Ag} = 0.5 *i.e.* 0.650, 0.577, and 0.527 for 1423 K, 1523 K, and 1623 K respectively for Ag-Cu melts.

The E^{XS}/RT in terms of Ag-composition for Ag-Cu alloys at various temperatures such as 1423 K, 1523 K and 1623 K calculated using Equation (19) are sighted in Figure 8. Obviously, E^{XS}/RT exhibit negative value at each concentration of Ag in the region x_{Ag} = 0.1 to 0.9 for each temperature under

consideration. Nevertheless, the negative value of E^{XS}/RT decrease when temperature rises from 1423 - 1623 K. This represents the degradation of the segregation in Ag-Cu melts from 1423 - 1623 K.

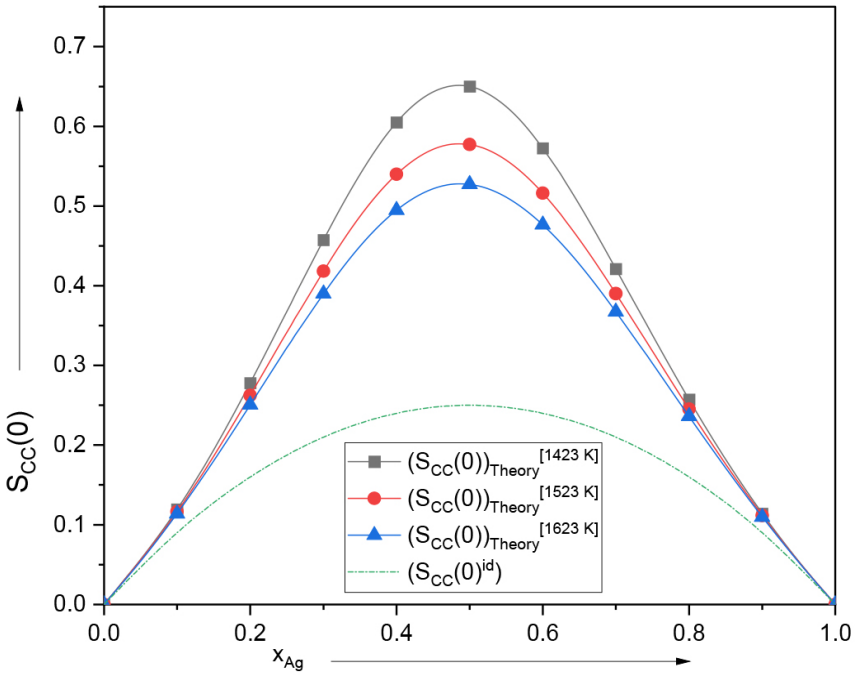

Figure 7. $S_{cc}(0)$ vs x_{Ag} for Ag-Cu melts at 1423, 1523 & 1623 K.

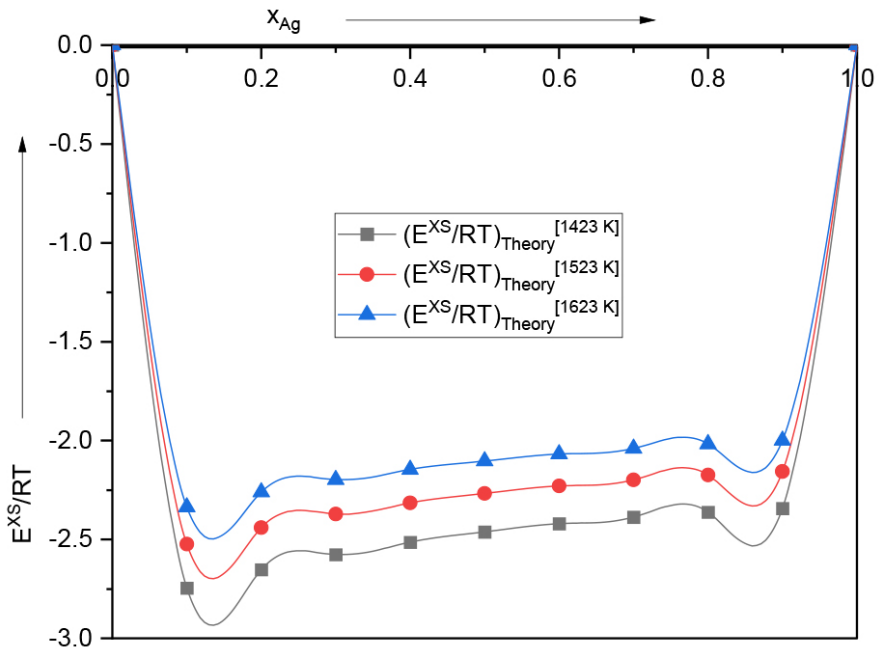

Figure 8. E^{XS}/RT vs x_{Ag} for Ag-Cu melts at 1423, 1523 & 1623 K.

The concertation as well as temperature dependence of α_1 for Ag-Cu melts calculated using Equation (18) are displayed in **Figure 9**. Obviously, at each

concentration, α_1 has positive value for each temperature *i.e.* 1423 K, 1523 K and 1623 K. The maximum value of α_1 is 0.0656 (at 1423 K) followed by 0.0601 (at 1523 K) and 0.0555 (at 1623 K) all at x_{Ag} = 0.5 which exhibit the symmetry in α_1 with respect to concentration for Ag-Cu melts in the temperature range 1423 - 1623 K. Again, the magnitude of α_1 decreases when temperature is raised from 1423 - 1623 K which signifies the degradation in the segregating behaviour of Ag-Cu melts for the temperatures from 1423 - 1623 K. Further, the small magnitude of α_1

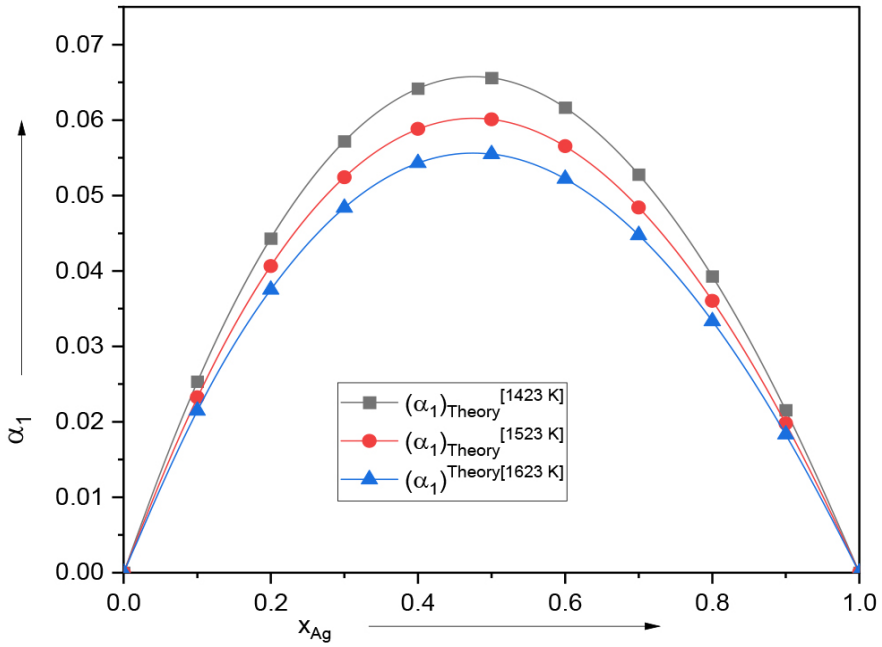

Figure 9. α_1 vs x_{Ag} for Ag-Cu melts at 1423, 1523 & 1623 K.

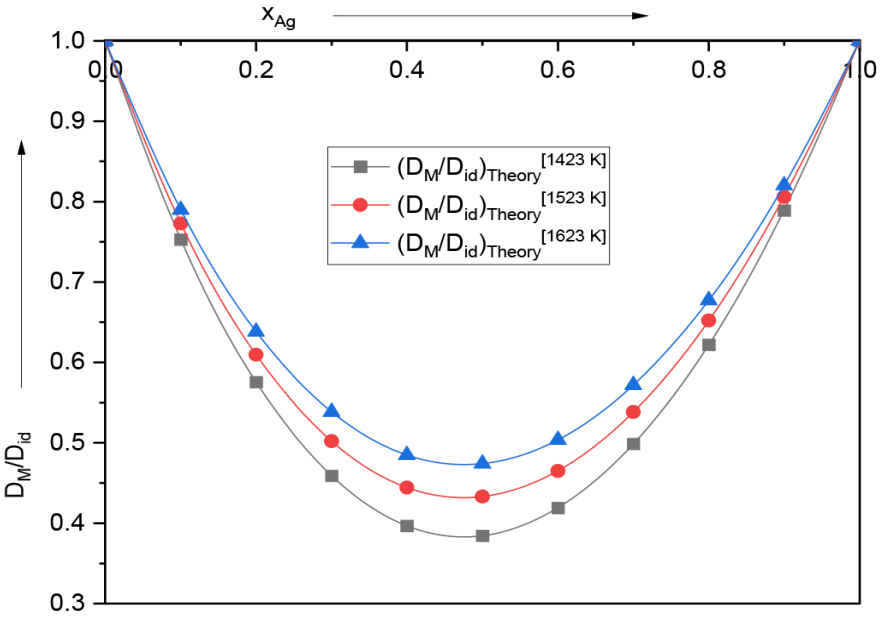

Figure 10. D_M/D_{id} vs x_{Ag} for Ag-Cu melts at 1423, 1523 & 1623 K.

confirms that Ag-Cu melt is a feebly segregating system in the temperature range, 1423 - 1623 K.

The theoretical values of D_M/D_{id} as a function of the Ag- concentration for Ag-Cu melts at 1423 K, 1523 K and 1623 K, calculated using Equation (20) are displayed in **Figure 10**. It is noticed that $D_M/D_{id} < 1$ in the composition region $0.1 \le x_{Ag} \le 0.9$ with minimum values of 0.3845, 0.4331, and 0.4741 at 1423 K, 1523 K, and 1623 K respectively at equiatomic composition, x_{Ag} = 0.5 for Ag-Cu melts. Therefore, with the rise in temperature from 1423 – 1623 K, the value of D_M/D_{id} rises at each composition which signifies the decrease in the segregating nature of Ag-Cu system when temperature rises from 1423 – 1623 K.

4. Conclusions

The present theoretical analysis successfully explains the mixing behaviour of Ag-Cu melts with respect to Ag-composition in the temperature region 1423 K to 1623 K. The results for thermodynamic, structural and transport properties suggest the homo-coordination in Ag-Cu melts in the temperature range 1423 - 1623 K and homo-coordination is maximum at x_{Ag} = 0.5. Again, Ag-Cu melts is a feebly segregating system and the order of segregation decreases when temperature rises from 1423 - 1623 K.

Therefore, MIVM approach is a reliable tool to explain theoretically the mixing properties of segregating alloys at the various temperatures. The MIVM is found to be a suitable model to explain G_M^E, G_M, activity, enthalpy etc. of binary melts like ordered, segregating and compound forming liquid alloys. Further, this model can be utilized to analyse the structural properties of multicomponent alloys. It is mentioned that MIVM is inadequate to explain the phase diagram of binary and multicomponent alloys. Therefore, MIVM may be combined with other sophisticated models like CALPHAD to study the phase diagram as well as thermodynamics of binary as well as multicomponent liquid alloys.

Author Contributions

Conceptualization, I. S. Jha and J. Mandal; methodology, N. K. Roy; validation, I.S. Jha, J. Mandal and A.K, Pandey; formal analysis, P. R. Deen; investigation, S. Kumari; writing original draft preparation, P. R. Deen & S. Kumari; writing-review and editing, N. K. Roy; visualization, I. S. Jha & A. K. Pandey; supervision, J. Mandal. All authors have read and agreed to published version of the manuscript.

Conflicts of Interest

The authors declare no conflicts of interest regarding the publication of this paper.

References

[1] Hultgren, R., Desai, P.D., Hawkins, D.T., Gleiser, M. and Kelley, K.K. (1973) Selected Values of the Thermodynamic Properties of Binary Alloys. ASM.

[2] Novakovic, R., Ricci, E., Giuranno, D. and Passerone, A. (2005) Surface and

Transport Properties of Ag-Cu Liquid Alloys. *Surface Science*, **576**, 175-187. https://doi.org/10.1016/j.susc.2004.12.009

[3] Witusiewicz, V., Hecht, U., Fries, S. and Rex, S. (2004) The Ag-Al-Cu Systempart I: Reassessment of the Constituent Binaries on the Basis of New Experimental Data. *Journal of Alloys and Compounds*, **385**, 133-143. https://doi.org/10.1016/s0925-8388(04)00676-0

[4] Singh, R.N. and Sommer, F. (1997) Segregation and Immiscibility in Liquid Binary Alloys. *Reports on Progress in Physics*, **60**, 57-150. https://doi.org/10.1088/0034-4885/60/1/003

[5] Fima, P. and Sobczak, N. (2010) Thermophysical Properties of Ag and Ag-Cu Liquid Alloys at 1098K to 1573K. *International Journal of Thermophysics*, **31**, 1165-1174. https://doi.org/10.1007/s10765-010-0798-5

[6] Kucharski, M., Fima, P., Skrzyniarz, P. and Przebinda-Stefanowa, W. (2006) Surface Tension and Density Cu-Ag, Cu-In and Ag-In Alloys. *Archives of Metallurgy and Materials*, **51**, 389-397.

[7] Tsai, Y., Hutabalian, Y. and Chen, S. (2025) Phase Diagrams and Microstructures Related to the Miscibility Gap of the Ag-Cu-Se System. *Journal of Alloys and Compounds*, **1036**, Article 181751. https://doi.org/10.1016/j.jallcom.2025.181751

[8] Jha, I.S., Koirala, I., Singh, B.P. and Adhikari, D. (2014) Concentration Dependence of Thermodynamic, Transport and Surface Properties in Ag-Cu Liquid Alloys. *Applied Physics A*, **116**, 1517-1523. https://doi.org/10.1007/s00339-014-8282-x

[9] Brillo, J., Lauletta, G., Vaianella, L., Arato, E., Giuranno, D., Novakovic, R., *et al.* (2014) Surface Tension of Liquid Ag-Cu Binary Alloys. *ISIJ International*, **54**, 2115-2119. https://doi.org/10.2355/isijinternational.54.2115

[10] Ohnuma, I., Miyashita, M., Anzai, K., Liu, X.J., Ohtani, H., Kainuma, R., *et al.* (2000) Phase Equilibria and the Related Properties of Sn-Ag-Cu Based Pb-Free Solder Alloys. *Journal of Electronic Materials*, **29**, 1137-1144. https://doi.org/10.1007/s11664-000-0004-9

[11] Ajayi, A.A., Oyeniyi, E. and Oshakuade, O.M. (2023) Bulk and Surface Properties of Liquid Ag-Cu, Ag-Sb and Cu-Sb Alloys. *Pramana*, **97**, Article No. 72. https://doi.org/10.1007/s12043-023-02536-x

[12] Tao, D.P. (2000) A New Model of Thermodynamics of Liquid Mixtures and Its Application to Liquid Alloys. *Thermochimica Acta*, **363**, 105-113. https://doi.org/10.1016/s0040-6031(00)00603-1

[13] Roy, N.K., Chaudhary, R.P., Vrind, N., Sahu, R.K., Mandal, J. and Jha, I.S. (2026) Microscopic Properties of BISN Melts at Various Temperatures by Molecular Interaction Volume Model. *AIP Conference Proceedings*, **3397**, Article 020002. https://doi.org/10.1063/5.0348363

[14] Roy, N.K., Vrind, N., Sahu, R.K., Mandal, J. and Jha, I.S. (2025) Prediction of the Alloying Behaviour of Ni-Pd Melts by Molecular Interaction Volume Model. *IOP Conference Series*: *Materials Science and Engineering*, **1334**, Article 012005. https://doi.org/10.1088/1757-899x/1334/1/012005

[15] Poizeau, S. and Sadoway, D.R. (2013) Application of the Molecular Interaction Volume Model (MIVM) to Calcium-Based Liquid Alloys of Systems Forming High-Melting Intermetallics. *Journal of the American Chemical Society*, **135**, 8260-8265. https://doi.org/10.1021/ja4013886

[16] Ding, G.H., Liang, L.M., Meng, P., Wang, L., Wang, Y.X., Wang, Y.J., *et al.* (2019) Application of the Molecular Interaction Volume Model to the Assessment of Thermodynamic

Properties of Liquid Zn-Bi Alloys. *Metallic Materials*, **57**, 55-60. https://doi.org/10.4149/km_2019_1_55

[17] Odusote, Y.A., Jabar, J.M., Bolarinwa, H.S. and Akinbisehin, A.B. (2019) Application of Molecular Interaction Volume Model in Separation of Ti-Al Alloys in Vacuum Distillation. *Vacuum*, **169**, Article 108885. https://doi.org/10.1016/j.vacuum.2019.108885

[18] Roy, N.K., Vrind, N., Bhagat, S.K., Prabhu, R., Mandal, J. and Jha, I.S. (2026) Temperature and Composition Reliance of the Mixing Properties of Fe-Mn Melts by Molecular Interaction Volume Model. *World Journal of Condensed Matter Physics*, **16**, 37-54. https://doi.org/10.4236/wjcmp.2026.163003

[19] Liang, L.M., Ding, G.H., Wang, Y.X. and Liu, Y. (2021) Thermodynamic Properties of Liquid Zn-Cd Alloys Investigated by the Molecular Interaction Volume Model. *Physics and Chemistry of Liquids*, **59**, 706-715. https://doi.org/10.1080/00319104.2020.1808655

[20] Liang, L.M., Ren, X., Wang, Y. Zhu, C. and Wang, Y.X. (2025) Thermodynamic-Guided Transport Properties of Liquid Pb-Bi Alloys via Molecular Interaction Modeling. *Journal of Phase Equilibria and Diffusion*, **46**, 366-374. https://doi.org/10.1007/s11669-025-01200-8

[21] Roy, N.K., Singh, A.P., Chaudhary, R.P., Mandal, J. and Jha, I.S. (2026) Theoretical Predictions of Thermodynamic Behavior for Cd-Tl Melts at Different Temperatures. *World Journal of Condensed Matter Physics*, **16**, 55-72. https://doi.org/10.4236/wjcmp.2026.163004

[22] Kong, L.X., Yang, B., Xu, B.Q., Li, Y.F., Li, L., *et al.* (2013) Application of Molecular Interaction Volume Model in Separation of Pb-Sn-Sb Ternary Alloy by Vacuum Distillation. *Transactions of Nonferrous Metals Society of China*, **23**, 2408-2415. https://doi.org/10.1016/s1003-6326(13)62748-x

[23] Odusote, Y.A. and Akindele, D.O. (2020) Estimation of Sn Activity in Ternary Lead-Free Sn-Ag-Au Alloys and its Subsystems. *FUOYE Journal of Pure and Applied Sciences*, **5**, 121-134.

[24] Sah, S.K., Jha, I.S. and Koirala, I. (2023) Theoretical Examination of Some Thermodynamic Properties in In-Bi-Sn Liquid Alloy and Its Sub-Binary Systems. *Journal of Electronic Materials*, **52**, 6350-6359. https://doi.org/10.1007/s11664-023-10571-y

[25] Bhatia, A.B. and Thornton, D.E. (1970) Structural Aspects of the Electrical Resistivity of Binary Alloys. *Physical Review B*, **2**, 3004-3012. https://doi.org/10.1103/physrevb.2.3004

[26] Bhatia, A.B. and Hargrove, W.H. (1974) Concentration Fluctuations and Thermodynamic Properties of Some Compound Forming Binary Molten Systems. *Physical Review B*, **10**, 3186-3196. https://doi.org/10.1103/physrevb.10.3186

[27] Warren, B.E. (1969) X-Ray Diffraction. Addition-Weseley.

[28] Cowley, J.M. (1950) An Approximate Theory of Order in Alloys. *Physical Review*, **77**, 669-675. https://doi.org/10.1103/physrev.77.669

[29] Singh, R.N. (1987) Short-Range Order and Concentration Fluctuations in Binary Molten Alloys. *Canadian Journal of Physics*, **65**, 309-325. https://doi.org/10.1139/p87-038

[30] Darken, L.S. (1967) Thermodynamics of Binary Metallic Solutions. *Transactions of the Metallurgical Society of AIME*, **239**, 80-89.

[31] Singh, A.P., Chaudhary, R.P., Kumari, R., Jha, I.S. and Mandal, J. (2022) Stability of Nak Liquid Alloys at Different Temperatures. *Materials Today: Proceedings*, **66**,

2251-2258. https://doi.org/10.1016/j.matpr.2022.06.097

[32] Sridhar, S. (2010) A Commentary on "Diffusion, Mobility and Their Interrelation through Free Energy in Binary Metallic Systems," L.S. Darken: Trans. AIME, 1948, Vol. 175, P. 184ff. *Metallurgical and Materials Transactions A*, **41**, 543-562. https://doi.org/10.1007/s11661-010-0177-7

[33] Iida, T. and Guthrie, R.I.L. (1988) The Physical Properties of Liquid Metals. Oxford University Press.